Biocatalytic Self-Assembly

Deutsche Ausgabe: DOI: 10.1002/ange.201500867
Internationale Ausgabe: DOI: 10.1002/anie.201500867

# Biocatalytic Pathway Selection in Transient Tripeptide Nanostructures**

*Charalampos G. Pappas, Ivan R. Sasselli, and Rein V. Ulijn**

***Abstract:*** *Structural adaption in living systems is achieved by competing catalytic pathways that drive assembly and disassembly of molecular components under the influence of chemical fuels. We report on a simple mimic of such a system that displays transient, sequence-dependent formation of supramolecular nanostructures based on biocatalytic formation and hydrolysis of self-assembling tripeptides. The systems are catalyzed by α-chymotrypsin and driven by hydrolysis of dipeptide aspartyl-phenylalanine-methyl ester (the sweetener aspartame, DF-OMe). We observed switch-like pathway selection, with the kinetics and consequent lifetime of transient nanostructures controlled by the peptide sequence. In direct competition, kinetic (rather than thermodynamic) component selection is observed.*

Living systems are exceptionally capable of altering their structures in response to changing situations, largely through molecular assembly and disassembly via competing catalytic pathways under the influence of chemical fuels. There is tremendous interest in developing man-made analogues of such systems, which provide insight into the workings of biology's remarkable ability to adapt to changing environments and may find use in future adaptive nanotechnologies.[1–7] Dynamic processes in living systems are regulated by balancing thermodynamic and kinetic aspects. The rapid responses required for biological survival are achieved through catalytic amplification, which enables dynamic change under otherwise constant conditions. Indeed, enzymes are increasingly used to activate or deactivate a variety of functions in designed, peptide-based nanostructures, including self-assembly.[8,9] Furthermore, nature's self-assembly systems operate away from equilibrium, facilitating "unfavorable" reactions by coupling them to hydrolysis of a high-energy molecular fuel. Most existing laboratory-based self-assembly processes[10–13] are designed with thermodynamics, rather than kinetics, in mind. Changes in environmental conditions, such as temperature, ionic strength, solvent, and pH value, result in thermodynamically driven self-assembly. In particular for supramolecular gels,[14,15] equilibrium is not always reached and consequently the self-assembly route is crucial in determining the final supramolecular architecture.[16] Kinetics may also be controlled by taking advantage of the catalytic production of self-assembly building blocks, as demonstrated using enzymatic[17] and chemical catalysis.[18] The first example of a chemically fuelled, non-equilibrium supramolecular system was demonstrated by Boekhoven et al., who showed that transient hydrogelation may be achieved by catalytic esterification (to form a gelator) and competing, thermodynamically favored hydrolysis of the ester group.[19] We recently demonstrated the chemically fuelled biocatalytic formation of peptide nanofibers which display dynamic instability based on transient formation (fuelled by ester hydrolysis) and degradation of an aromatic dipeptide amphiphile.[20] Transient self-assembling nanostructures have also been achieved by controlled protonation and consequent disassembly, using dynamically controlled pH gradients.[21]

Sequence-dependent function may be found even in very short peptide sequences.[22–26] Thus, a system where different peptides are formed through competing pathways provides interesting opportunities for nanostructures with adaptive functions. Herein, we demonstrate peptide-sequence-dependent kinetic pathway selection in the chemically fuelled biocatalytic self-assembly of tripeptides. We show that these systems demonstrate transience, with the lifetime of the nanostructures dictated by the peptide sequence. We stress that the approach used in this Communication is conceptually different from our previous work on equilibrium-driven enzymatic self-assembly.[27–29] In that work, the thermodynamic stabilization of the peptide reaction product drives the reaction and the equilibrium situation represents the assembled state, that is, equilibrium-driven formation of peptide nanostructures. In the current approach we deliberately focus on peptides that do not assemble at equilibrium, that is, we operate them under conditions where self-assembly is not favored. This point is key to achieving transience because, as demonstrated previously by us[20] and others,[19] nanostructure formation should be unfavorable at equilibrium.

Therefore, to produce transient structures, a "poor assembler" is required, necessitating a balance of attractive and repulsive forces within one molecule. In addition, the peptide

[*] C. G. Pappas, I. R. Sasselli, Prof. R. V. Ulijn
WestCHEM/Department of Pure and Applied Chemistry
University of Strathclyde
295 Cathedral Street, Glasgow G1 1XL (UK)
E-mail: rein.ulijn@strath.ac.uk
C. G. Pappas, Prof. R. V. Ulijn
Advanced Science Research Centre (ASRC)
City University of New York
85 St Nicholas Terrace, New York, NY, 10031 (USA)
E-mail: rein.ulijn@asrc.cuny.edu

[**] We would like to thank C. Irving for the DOSY NMR experiments, P. Keating, D. Kalafatovic, and A. Primikyri for the HPLC and mass spectral analysis, M. Mullin for the TEM experiments, and P. Frederix for the discussions with the FTIR experiments. The research leading to these results has received funding from the European Research Council under the European Union's Seventh Framework Programme (FP7/2007–2013) EMERgE/ERC Grant Agreement Number 258775. C.G.P. would like to thank Linn Products Ltd. for funding.

Supporting information for this article is available on the WWW under http://dx.doi.org/10.1002/anie.201500867.

  

should be a good substrate for the enzymatic reaction. As the enzyme, we chose α-chymotrypsin which has previously been used in biocatalytic self-assembly[20] and has a well-documented preference for aromatic residues at the C terminus. Conveniently, the artificial sweetener aspartame, a dipeptide methyl ester (DF-OMe), used as a sugar substitute in some foods and beverages,[30,31] is a potential substrate for α-chymotrypsin that also provides phenylalanine (F) in position 2 to ensure the peptides have a propensity to aggregate and a conflicting aspartic acid (D) at the N-terminus position. For the purposes of this work, aspartame provides a low-cost, water-soluble activated precursor for the formation of transient nanostructures. The third amino acid is used to regulate the properties of the material formed by using a range of amino acid amides (Scheme 1) to form DFX-$NH_2$.

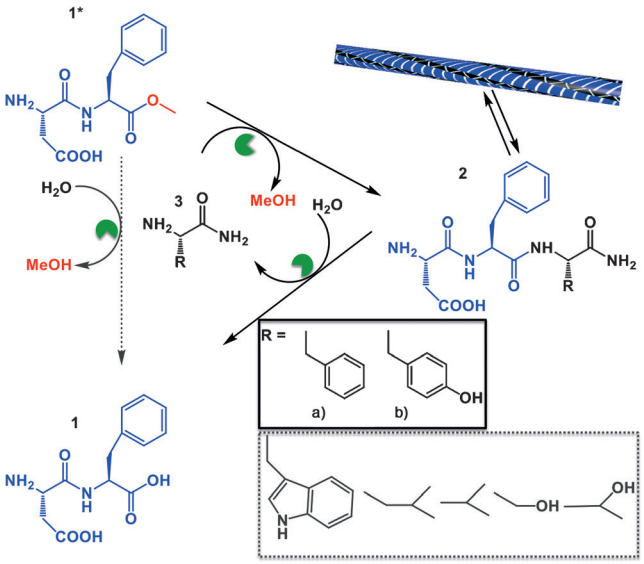


***Scheme 1.*** Sequence-controlled pathway selection in transient biocatalytic self-assembly from a dipeptide precursor (aspartame; **1***) with different amino acid amides in the presence of α-chymotrypsin to form the temporary tripeptide hydrogelator, which may be also hydrolyzed by the same enzyme.

It is anticipated that transient supramolecular architecture and hydrogel formation arises from aromatic stacking interactions between the aromatic amino acid residues and hydrogen bonding between the tripeptide backbones.[23,32,33]

Thus, starting from aspartame (**1***; DF-OMe) and a range of amino acid amides (X-$NH_2$, where X = W, Y, F, L, V, S, or T) with α-chymotrypsin[18] as the catalyst, a range of potential tripeptide amides may be formed (DFX-$NH_2$). The forward reaction, resulting in peptide formation (**1***→**2**, Scheme 1) was enabled by α-chymotrypsin-catalyzed transacylation.[20,34,35] Provided that self-assembly is thermodynamically disfavored under the conditions used, this should lead to the formation of **2** (which exists only transiently), which is subsequently hydrolyzed to **1** (Scheme 1). It should be noted that transient supramolecular structures would only exist if the amide bond formation (**1***→**2**) is faster than the hydrolysis (**1***→**1**) and if amide hydrolysis (**2**→**1**) is slow.

Remarkably, we observed a substantial difference in pathway selection depending on the choice of the amino acid amide nucleophile. In the presence of W, L, V, S, and T no gelation was observed. Using high-performance liquid chromatography (HPLC), **2** was not detected, indicating its transient existence was either of a very short duration and immediately hydrolyzed or did not occur at all. Instead, hydrolysis towards the formation of DF (**1**) occurred within 30 min. This is unexpected because in previous work it has been shown that a variety of amino acid amides (L, V, S) may be used as nucleophiles with high yields (60–80%) in chymotrypsin-catalyzed peptide synthesis by transacylation,[34] although in that work the polymeric peptide product was thermodynamically stable, therefore, the **2**→**1** reaction was not favored.

In contrast, peptide formation and self-assembly was obtained when using F-$NH_2$ (**3a**) or Y-$NH_2$ (**3b**). We observed instant hydrogel formation after gently vortexing and sonicating (gelation was observed inside the sonication bath). Note that W-$NH_2$ did not give rise to transient gelation, despite the fact that it has previously been identified as a good candidate for self-assembly.[23] It is noteworthy that without sonication (only vortexing) of the precursor solution, gelation was observed after 5 min, indicating that ultrasonic energy enhance the kinetics of the system. No gelation was observed without the addition of chymotrypsin into the system. Digital photos of the macroscopic transitions can be found in Figure S1 in the Supporting Information. Monitoring the DF-OMe/F-$NH_2$ reaction by HPLC, it was identified that the tripeptide product (**2a**) had the highest conversion within 30 min. Gradually, the peptide hydrolyzed, giving rise to the formation of DF (**1**), while after 72 h the percentage of **2a** (DFF-$NH_2$) was found to be around 10% (Figure 1a). This value represents the equilibrium conversion for DFF-$NH_2$ (which is clearly below the critical gelation concentration). Replacing phenylalanine (F-$NH_2$, **3a**) with tyrosine amide (Y-$NH_2$, **3b**) we found that the lifetime of the gel could be reduced significantly, from 24 to 4 h. HPLC analysis of the reaction revealed that DFY-$NH_2$ (**2b**) reached complete conversion after 30 min. After 2 h the tripeptide was reduced to 40% and it completely disappeared after 10 h (Figure 1b), showing that this peptide has a lower propensity for self-assembly than DFF-$NH_2$. It should be noted that by using mass spectroscopy we detected the formation of the dimeric product (DFDF, $m/z$ 541.83) as well as some diketopiperazine (DKP, $m/z$ 263.1131) present in the starting material, however only in low abundance. The HPLC chromatographs and mass spectra of all the reactions at different time points are available in the Supporting Information (Figure S2–10).

These results indicate that sequence-specific interactions played a major role for the formation of the transient product and may be used to achieve a pathway switch. We propose that the formed nanofibers observed for **2a** and **2b** are potentially less prone to enzymatic hydrolysis in their assembled state (i.e. delaying the reaction **2**→**1**).

To further investigate the temporary formation and degradation of the peptide nanostructures, transmission electron microscopy (TEM) was used at different time points. Figures 1c,h show the precursor **1***. In the case of

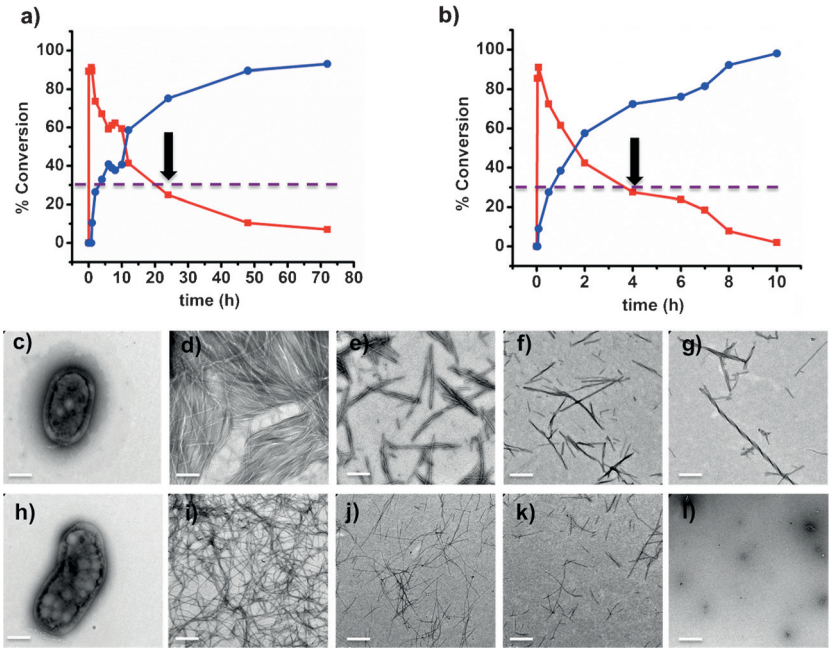


***Figure 1.*** HPLC analysis of a) **2a** and b) **2b** product formation and degradation with the red line representing DFF-$NH_2$ (in (a)) or DFY-$NH_2$ (in (b)) and the blue line representing DF (**1**). The black arrow represents the gel-to-sol transition and the dotted purple line the critical aggregation concentration. c–g) TEM images of aspartame (**1**$^*$) and tripeptide product **2a** (DFF-$NH_2$) after 0.08, 6, 48, and 72 h, respectively. h–l) TEM images of aspartame **1**$^*$ and tripeptide product **2b** (DFY-$NH_2$) after 0.08, 4, 8, and 24 h, respectively. Scale bar in (c–l) = 500 nm.

DFF-$NH_2$, early-stage (0.08 h) TEM images show an entangled fibrillar network and the length of the fibers was found to be $< 5$ μm (Figure 1 d). After 6 h, considerable shortening of the fibers was observed (Figure 1 e). At this stage, the material remained in the gel phase because of the presence of 70% of the tripeptide. After 48 h we noticed further shortened fibers of approximately 1-2 μm in length (Figure 1 f), where the concentration of the tripeptide was found to be around 20%. Finally after 72 h, at a conversion of approximately 10%, short fibers remained visible (Figure 1 g). The formation and shortening of the supramolecular architecture provides strong evidence of a dynamically unstable system. To investigate the possibility of repeated transient supramolecular reconfiguration and gelation, 1 equivalent (20 mM) of aspartame (**1**$^*$) was added into the system after 24 h, upon which hydrogel formation was observed after gently vortexing and sonicating. This could be repeated for up to three cycles, however the conversion into the transient tripeptide product reduced (to 60 and 30%, respectively), which was most likely related to the accumulation of DF (**1**) in the system (Figures S11–12). TEM was also used to probe the structural changes at the microscopic level in the case of DFY-$NH_2$ (**2b**). Initially, TEM revealed an entangled fibrillar network of approximately 7–8 μm of length (Figure 1 i). After 4 h the fibers broke down to about 3 μm as the tripeptide remained in the gel phase with a concentration 30%. After 8 h, further shortening of fibers was observed and after 24 h spherical aggregates were formed (Figure 1 l). These spherical aggregates can be attributed to the formation of DF (**1**) as a result of complete hydrolysis of **2b**.

To probe the nature of the temporary supramolecular interactions we used FTIR to follow the transient β-sheet-like arrangement of the amide groups.[23] No hydrogen-bonding-type interactions were found for **1**$^*$ in the amide region of the spectrum indicating that the structures observed by TEM are disorganized aggregates.

Upon transacylation and assembly of **2a** a strong band at 1648 $cm^{-1}$ was identified, suggesting the formation of a hydrogen-bonded network with limited long-range order.[36,37] Additionally, a band assigned to the carboxylate group of the sidechain of aspartic acid was found at 1588 $cm^{-1}$. Gradually, after 6 h the intensity of the band at 1648 $cm^{-1}$ decreased and after 72 h was lost (Figure 2 a). After this time, the spectrum also contained a small contribution at higher wavenumbers of the 1588 $cm^{-1}$ band compared to the aspartame spectrum. In contrast, FTIR analysis of **2b** revealed a strong band at 1624 $cm^{-1}$ suggesting formation of more ordered hydrogen-bonding-type interactions between the tripeptides. Additionally, a band appeared at 1647 $cm^{-1}$, as previously detected for **2a**. After 4 h, the intensity of the band for the β-sheet-like arrangement was decreased, with the band disappearing after 24 h (Figure 2 b). The FTIR spectrum of 1 mg $mL^{-1}$ of α-chymotrypsin as a control experiment is shown in Figure S13, and shows a very weak band at 1624 $cm^{-1}$ for hydrogen-bonding-type interactions.

To further investigate the transient supramolecular reconfiguration and assembly of **2b**, we used diffusion ordered NMR spectroscopy (DOSY NMR). It was not possible to investigate **2a** by the same method as a result of formation of some insoluble material. Following the reaction, it was revealed that the hydrodynamic radius of the molecule became bigger as the diffusion of **2b** decreased (5 $m^2 s^{-1}$). With subsequent amide hydrolysis, the diffusion constant increased and was found to be close to that of the starting material (approximately 6 $m^2 s^{-1}$; Figure S14).

The structural differences between **2a** and **2b** in terms of supramolecular self-assembly and the control of the kinetics by chemical design prompted us to investigate direct competition between the nucleophiles (**2a**, **2b**) in the presence of the enzymatic catalyst and the acyl donor. Aspartame (**1**$^*$; 20 mM) and the nucleophiles (40 mM; 20 mM of each) in the presence of α-chymotrypsin (1 mg) were employed. As shown in Figure 3 a, after 1 hour of the competition reaction, **2b** was formed preferentially in a yield conversion of 70%, with 30% of **2a**. Gradually, both of the tripeptides started to break down and after 48 h the concentration of **2b** was found to be 20%, whereas **2a** almost disappeared (approximately 3%).

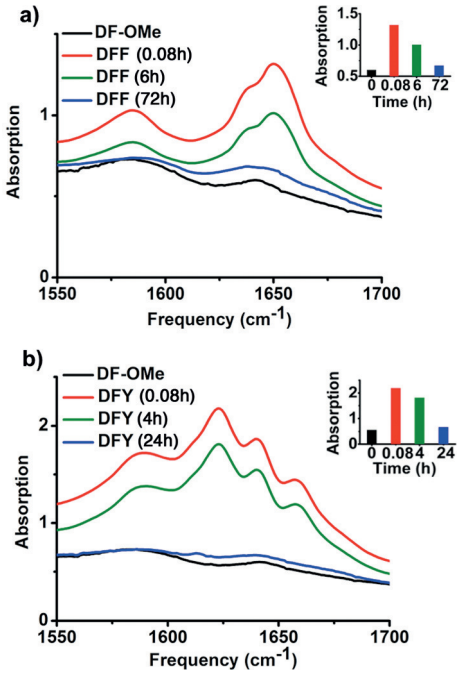


***Figure 2.*** a,b) FTIR spectra in $D_2O$ of aspartame (**1***, DF-OMe; 20 mM) in sodium phosphate buffer (100 mM; pH 8) with either a) **2a** (DFF-$NH_2$) or b) **2b** (DFY-$NH_2$), recorded at different time points. Inset in (a) shows a plot of the absorption values at 1648 $cm^{-1}$ for **2a** an d in (b) at 1624 $cm^{-1}$ for **2b**.

The FTIR spectrum of the competition experiments revealed a band at 1624 $cm^{-1}$, which was previously detected for **2b** (Figure 3b). Figure S15 shows time-dependent FTIR experiments. TEM images revealed sequential fiber formation and degradation (Figure 3c–f) with the fibers looking thinner and less twisted, similar to the fibrillar nature of **2b**. It is not possible to say with certainty whether **2a** and **2b** form co-assembled structures or form discrete structures. The remarkably similar degradation profile for both suggests that the degradation mechanisms are linked. However, it is clear from our results that **2b** is preferentially formed as it is formed in a higher yield, so in terms of molecular composition it outcompetes **2a**. These data therefore suggest that kinetic (rather than thermodynamic)[27–29] selection of nanostructures occurs. Additional TEM images for the fibrillar formation and degradation of **2a** and **2b** and for the competition experiments are available in Figures S16–S18. Histograms with the fibrillar length distribution for all the TEM experiments can be found in Figure S19.

In summary, we have demonstrated sequence-dependent pathway selection in a non-equilibrium biocatalytic assembly, a reaction driven by the hydrolysis of the methyl ester in the sweetener aspartame (DF-OMe). These dynamically unstable systems could be refueled several times by addition of aspartame. In the direct competition between F-$NH_2$ and Y-$NH_2$ the kinetically preferred product (DFY-$NH_2$) rather than the most stable product (DFF-$NH_2$) dominates, demonstrating kinetic, rather than thermodynamic, selection of nanostructures. We demonstrate control of the kinetics and consequently the lifetime of the nanostructures formed by chemical design. This work provides a step toward a better understanding of structural adaption in biological systems and opens up new opportunities to create supramolecular systems for non-equilibrium motility and shape control.

**Keywords:** biocatalysis · hydrogel · nanostructures · peptides · self-assembly

**How to cite:** *Angew. Chem. Int. Ed.* **2015**, *54*, 8119–8123
*Angew. Chem.* **2015**, *127*, 8237–8241

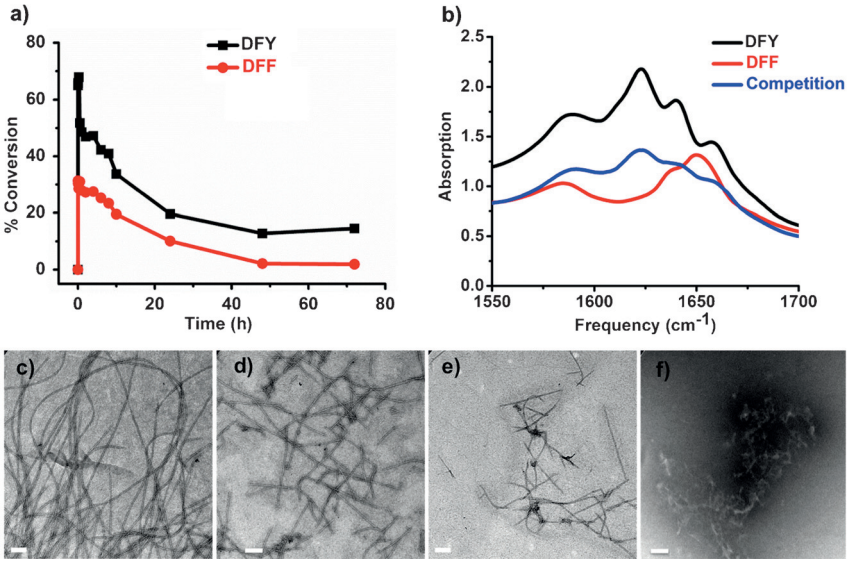


***Figure 3.*** a) HPLC of the competition experiment between **2a** and **2b** in phosphate buffer pH 8. b) FTIR of **2a**, **2b**, and mixture after 0.08 h. c–f) TEM images of the mixture after 0.08, 4, 24, and 72 h, respectively. Scale bar = 500 nm.

[1] S. C. Warren, O. Guney-Altay, B. A. Grzybowski, *J. Phys. Chem. Lett.* **2012**, *3*, 2103–2111.
[2] S. Mann, *Angew. Chem. Int. Ed.* **2013**, *52*, 155–162; *Angew. Chem.* **2013**, *125*, 166–173.
[3] S. N. Semenov, A. J. Markvoort, T. F. de Greef, W. T. Huck, *Angew. Chem. Int. Ed.* **2014**, *53*, 8066–8069; *Angew. Chem.* **2014**, *126*, 8204–8207.
[4] J. Li, P. Nowak, S. Otto, *J. Am. Chem. Soc.* **2013**, *135*, 9222–9239.
[5] A. Grinthal, J. Aizenberg, *Chem. Soc. Rev.* **2013**, *42*, 7072–7085.
[6] J. M. P. Gutierrez, T. Hinkley, J. W. Taylor, K. Yanev, L. Cronin, *Nat. Commun.* **2014**, *5*, 5571–5579.
[7] S. N. Semenov, A. S. Y. Wong, R. M. van der Made, S. G. J. Postma, J. Groen, H. W. H. van Roekel, T. F. A. de Greef, W. T. Huck, *Nat. Chem.* **2015**, *7*, 160–165.
[8] Y. Kuang, J. F. Shi, J. Li, D. Yuan, K. A. Alberti, Q. B. Xu, B. Xu, *Angew. Chem. Int. Ed.* **2014**, *53*, 8104–8107; *Angew. Chem.* **2014**, *126*, 8242–8245.
[9] Q. G. Wang, Z. M. Yang, X. Q. Zhang, X. D. Xiao, C. K. Chang, B. Xu, *Angew. Chem. Int. Ed.* **2007**, *46*, 4285–4289; *Angew. Chem.* **2007**, *119*, 4363–4367.

[10] G. M. Whitesides, M. Boncheva, *Proc. Natl. Acad. Sci. USA* **2002**, *99*, 4769 – 4774.
[11] R. M. Capito, H. S. Azevedo, Y. S. Velichko, A. Mata, S. I. Stupp, *Science* **2008**, *319*, 1812 – 1816.
[12] J. M. Lehn, *Science* **1993**, *260*, 1762 – 1763.
[13] T. Aida, E. W. Meijer, S. I. Stupp, *Science* **2012**, *335*, 813 – 817.
[14] W. Edwards, D. K. Smith, *J. Am. Chem. Soc.* **2013**, *135*, 5911 – 5920.
[15] P. Terech, R. G. Weiss, *Chem. Rev.* **1997**, *97*, 3133 – 3160.
[16] J. Raeburn, A. Zamith Cardoso, D. J. Adams, *Chem. Soc. Rev.* **2013**, *42*, 5143 – 5156.
[17] A. R. Hirst, S. Roy, M. Arora, A. K. Das, N. Hodson, P. Murray, S. Marshall, N. Javid, J. Sefcik, J. Boekhoven, J. H. van Esch, S. Santabarbara, N. T. Hunt, R. V. Ulijn, *Nat. Chem.* **2010**, *2*, 1089 – 1094.
[18] J. Boekhoven, J. M. Poolman, C. Maity, F. Li, L. van der Mee, C. B. Minkenberg, E. Mendes, J. H. van Esch, R. Eelkema, *Nat. Chem.* **2013**, *5*, 433 – 437.
[19] G. J. Boekhoven, A. M. Brizard, K. N. Kowlgi, G. J. Koper, R. Eelkema, J. H. van Esch, *Angew. Chem. Int. Ed.* **2010**, *49*, 4825 – 4828; *Angew. Chem.* **2010**, *122*, 4935 – 4938.
[20] S. Debnath, S. Roy, R. V. Ulijn, *J. Am. Chem. Soc.* **2013**, *135*, 16789 – 16792.
[21] T. Heuser, A. K. Steppert, C. Molano Lopez, B. Zhu, A. Walther, *Nano Lett.* **2015**, *15*, 2213 – 2219.
[22] C. M. Rufo, Y. S. Moroz, O. V. Moroz, J. Stöhr, T. A. Smith, X. Hu, W. F. DeGrado, I. V. Korendovych, *Nat. Chem.* **2014**, *6*, 303 – 309.
[23] P. M. J. W. Frederix, G. Scott, Y. Abul-haija, D. Kalafatovic, C. G. Pappas, N. Javid, N. Hunt, R. V. Ulijn, T. Tuttle, *Nat. Chem.* **2014**, *7*, 30 – 37.
[24] M. Reches, E. Gazit, *Science* **2003**, *300*, 625 – 627.
[25] J. Naskar, G. Palui, A. Banerjee, *J. Phys. Chem. B* **2009**, *113*, 11787 – 11792.
[26] J. M. Slocika, R. R. Naik, *Chem. Soc. Rev.* **2010**, *39*, 3454 – 3463.
[27] R. J. Williams, A. M. Smith, R. Collins, N. Hodson, A. K. Das, R. V. Ulijn, *Nat. Nanotechnol.* **2009**, *4*, 19 – 24.
[28] S. K. Nalluri, R. V. Ulijn, *Chem. Sci.* **2013**, *4*, 3699 – 3705.
[29] S. K. Nalluri, C. Berdugo, N. Javid, P. W. Frederix, R. V. Ulijn, *Angew. Chem. Int. Ed.* **2014**, *53*, 5882 – 5887; *Angew. Chem.* **2014**, *126*, 5992 – 5997.
[30] "Discovery of Aspartame": R. H. Mazur in *Aspartame: Physiology and Biochemistry*, (Eds.: L. D. Stegink, L. J. Filer, Jr.), Marcel Dekker, New York, **1984**, pp. 3 – 9.
[31] J. Suez, T. Korem, D. Zeevi, G. Zilberman-Schapira, C. A. Thaiss, O. Maza, D. Israeli, N. Zmora, S. Gilad, A. Weinberger, Y. Kuperman, A. Harmelin, I. Kolodkin-Gal, H. Shapiro, Z. Halpern, E. Segal, E. Elinav, *Nature* **2014**, *584*, 181 – 186.
[32] S. Marchesan, C. D. Easton, F. Kushkaki, L. Waddington, P. G. Hartley, *Chem. Commun.* **2012**, *48*, 2195 – 2197.
[33] S. Marchesan, L. Waddington, C. D. Easton, D. A. Winkler, L. Goodall, J. Forsythe, P. G. Hartley, *Nanoscale* **2012**, *4*, 6752 – 6760.
[34] J. Fastrez, A. R. Fersht, *Biochemistry* **1973**, *12*, 2025 – 2034.
[35] X. Qin, W. Xie, S. Tian, J. Cai, H. Yuan, Z. Yu, G. L. Butterfoss, A. C. Khuong, R. A. Gross, *Chem. Commun.* **2013**, *49*, 4839 – 4841.
[36] S. Fleming, P. M. J. W. Frederix, I. S. Sasselli, *Langmuir* **2013**, *29*, 9510 – 9515.
[37] A. Barth, C. Zscherp, *Q. Rev. Biophys.* **2002**, *35*, 369 – 430.

Received: January 29, 2015
Revised: April 3, 2015
Published online: May 26, 2015

  